Thermal expansion of single-walled carbon nanotube (SWNT) bundles: X-ray diffraction studies

Yutaka Maniwa,[1] Ryuji Fujiwara,[1] Hiroshi Kira,[1] Hideki Tou,[1] Hiromichi Kataura,[1] Shinzo Suzuki,[2] Yohji Achiba,[2] Eiji Nishibori,[3] Masaki Takata,[3] Makoto Sakata,[3] Akihiko Fujiwara,[4] and Hiroyoshi Suematsu[4,*]

[1]*Department of Physics, Tokyo Metropolitan University, Minami-osawa, Hachi-oji, Tokyo, 192-0397, Japan*
[2]*Department of Chemistry, Tokyo Metropolitan University, Minami-osawa, Hachioji, Tokyo 192-0397, Japan*
[3]*Department of Applied Physics, Nagoya University, Nagoya 464-8603, Japan*
[4]*Department of Physics, School of Science, University of Tokyo, 7-3-1 Hongo, Bunkyo-ku, Tokyo 113-0033, Japan*
(Received 28 May 2001; revised manuscript received 20 August 2001; published 28 November 2001)

Thermal expansion coefficient in single-walled carbon nanotube bundles was determined as $(-0.15 \pm 0.20) \times 10^{-5}$ (1/K) for the tube diameter and $(0.75 \pm 0.25) \times 10^{-5}$ (1/K) for the triangular lattice constant by means of x-ray scattering between 300 K to 950 K. The value for the intertube gap was $(4.2 \pm 1.4) \times 10^{-5}$ (1/K), which is larger than 2.6×10^{-5} (1/K) for the c-axis thermal expansion in graphite. The results reveal the presence of a remarkably larger lattice anharmonicity in nanotube bundles than that of graphite. The small value for the tube diameter is consistent with the seamless tube structure formed by a strong covalent bond between carbon atoms comparable to that in graphite.

Single-walled carbon nanotubes (SWNTs) can be obtained, for example, in soot after arc-discharge or laser ablation of graphite containing metal catalyst.[1–5] Transmission electron microscopy (TEM) and x-ray diffraction (XRD) measurements of the soot clarified that the tubes are close-packed into bundles and form a triangular lattice.[4] Thermal expansion of the lattice constant and tube diameter is interesting because it gives us the nature of carbon-carbon bond and intertube interaction in the SWNT bundles. However little has been known so far experimentally. In the present note, we report, to the best of our knowledge, for the first time a determination of the thermal expansion coefficient for both the tube diameter and triangular lattice constant of an SWNT bundle by means of X-ray diffraction (XRD).

The soot containing SWNTs was prepared by a laser ablation of a carbon rod including a Ni-Co catalyst.[6] The obtained soot was purified by oxidation in H_2O_2 solution for two hours. After that, the sample was treated in hydrochloric acid to remove the catalyst. XRD data were collected using a synchrotron radiation source at beam line BL02B2 of SPring-8 and BL1B of KEK PF in Japan. The x-ray wavelength is 1.00 Å. In the first measurement, the sample was placed in a furnace with a beryllium window and evacuated during the measurement. In the second measurement where the temperature was controlled using a heat-gun, the sample was sealed in a glass capillary after being well evacuated at ~ 800 K.

Figure 1 shows the temperature (T) dependence of the XRD patterns in the first measurement. On the large background signal, we can see diffraction peaks due to the SWNT bundles. The (10) reflection from the triangular lattice shows a strong T-dependence. The peak intensity, which was normalized by the (002) reflection of impurity graphite, increases rapidly above 700 K with increasing T, as shown in Fig. 2. The onset of the (10) peak correspondingly shifts toward the lower 2θ side. Such behaviors are well understood by desorption of the materials, such as O_2, N_2, H_2O, and other hydrocarbons, from the bundles with increasing T.[7–9] When the temperature was lowered, the peak intensity

was almost constant because the desorption has almost completed. After this measurement, the sample was heated again. The XRD patterns, in this case, were very similar to those for the decreasing temperature, as expected.

Figure 3 shows the T-dependence of XRD patterns for the well heat-treated sample sealed within the capillary, where Q is the amplitude of the scattering wave vector defined by $Q = 4\pi \sin\theta/\lambda$. Because the sample has been well heated under a dynamic vacuum, the XRD patterns were essentially the same for the increasing and decreasing T. The graphite (002) peak of the impurity shows a remarkable T-dependence and the estimated thermal expansion coefficient of interlayer spacing is 2.6×10^{-5} (1/K), consistent with reported values for graphite.[10] In contrast, that of the SWNT sample may be found to be very weak, indicating that the thermal expansion
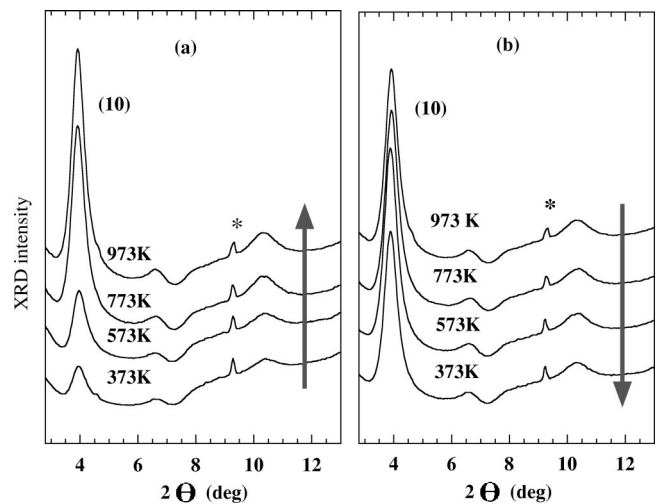

FIG. 1. Temperature dependence of XRD patterns in an SWNT bundle. The sample was placed in a furnace and evacuated to $\sim 10^{-6}$ Torr during the measurements. The x-ray wavelength is $\lambda = 1.0025$ Å. The peaks denoted by * are not due to the sample. Left and right figures show the measurements performed with increasing and decreasing temperature, respectively.
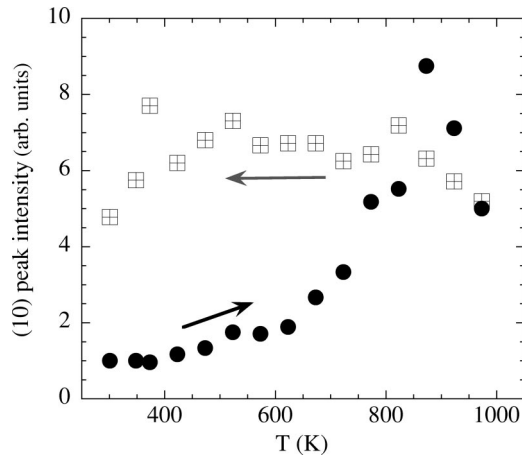
FIG. 2. The (10) peak intensity, normalized by the (002) peak intensity of graphite contained in the sample as an impurity, as a function of the sample temperature.

FIG. 4. Demonstration how to construct the simulated XRD pattern. Dashed line shows the squared zeroth-Bessel function. Bottom is the Bragg peak broadened by an appropriate amount.

of the SWNT bundle is much smaller than that for the graphite interlayer spacing.

Now, we simulate the XRD patterns of SWNT bundle in order to estimate the thermal expansion coefficient for the tube diameter and lattice constant. Here we use a homogeneous charged cylinder model for each tube, which is closed-packed into a triangular lattice.[4] It should be noted that this model cannot include the "in-plane" carbon-carbon bond structures, although it can reproduce the low Q diffraction intensity which gives us information on the tube diameter and lattice constants.

Figure 4 demonstrates how to obtain the XRD pattern from the simulation. The diffracted intensity is a multiplication of the tube form factor, Bragg peak intensity, and Lorentz factor. In the SWNT materials, the Bragg peaks are so broad that the resultant XRD pattern is strongly modulated by the tube form factor given by the zeroth-Bessel function, $J_0(RQ)$. Therefore, because the Bessel function has the nodes whose position is inversely proportional to the tube diameter $2R$ as shown in Fig. 4, the dips (Q_{dip}) in the ob-
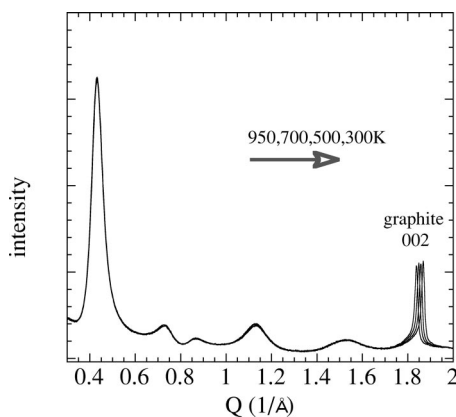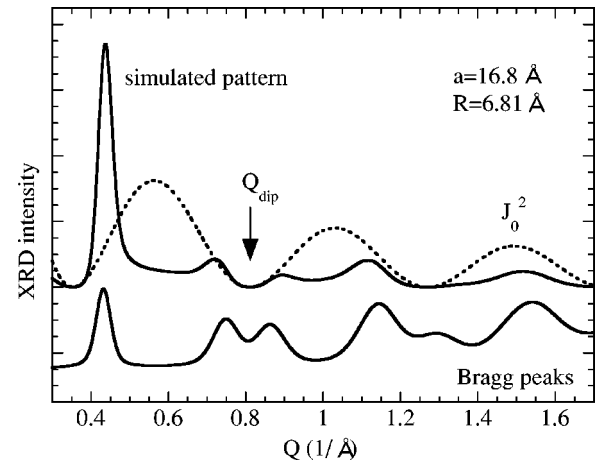
served pattern, corresponding to the nodes of $J_0(RQ)$, can give us the mean diameter with an accuracy of $\sim 0.1\%$. Figure 5 shows the T-dependence of Q_{dip}, giving $\alpha_D = (-0.15 \pm 0.20) \times 10^5$ (1/K) for the thermal expansion coefficient of the tube diameter. This is compared with the in-plane values, $(0 \pm 0.1) \times 10^5$ (1/K) in multiwalled carbon nanotube[11] in the same temperature domain, and also those for the in-plane thermal expansion in graphite.[10]

Assuming the zero thermal expansion for the tube diameter, we simulated the XRD patterns for several values for the thermal expansion coefficient for the triangular lattice constant. From the comparison with those taken at 300 K and 950 K experimentally, we obtained $\alpha_L = (0.75 \pm 0.25) \times 10^{-5}$ (1/K) as the most probable value for the averaged thermal expansion coefficient between 300 K and 950 K. The comparison between the simulated patterns and the observed ones is shown in Fig. 6.
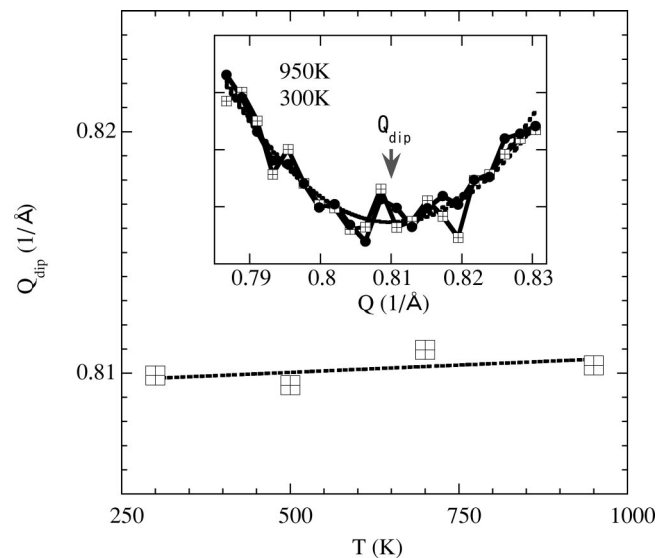

FIG. 3. Temperature dependence of XRD patterns in SWNT bundle. The sample was sealed within a glass tube after well evacuated at ~ 800 K. The x-ray wavelength is $\lambda = 1.0002$ Å. The measurements were performed with decreasing temperature.

FIG. 5. Temperature dependence of the Q_{dip} around $Q = 0.8$ (1/Å), corresponding to the node of the tube form factor, J_0. Inset shows examples of the observed data around $Q = 0.8$ (1/Å). The Q_{dip} was determined by a least-squared fit to the data.
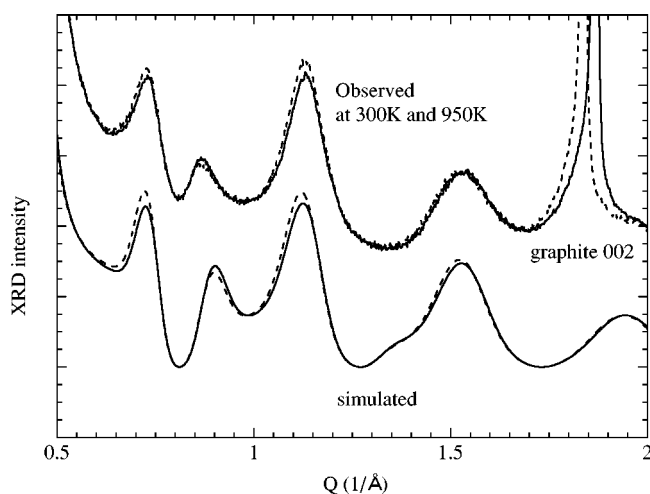
FIG. 6. Comparison of the observed data at 300 K and 950 K with simulated patterns, where the thermal expansion of the tube diameter and lattice constant were chosen as 0×10^{-5} (1/K) and 0.75×10^{-5} (1/K), and the lattice constant and the tube diameter are 16.60 Å and 13.62 Å at 300 K, respectively.

The estimated absolute values for the tube diameter and lattice constant in this simulation are $2R = 13.62 \pm 0.01$ Å and $a = 16.6 \pm 0.1$ Å at 300 K, respectively. The obtained tube diameter is consistent with a rough evaluation from the radial breathing mode in Raman spectra, ~ 14 Å. The inter-tube gap, $d = a - 2R$, is 3.0 Å. The corresponding thermal expansion for the gap is estimated to be $\alpha_g = 4.2 \times 10^{-5}$ (1/K), using a relation $\alpha_L = (2R\alpha_D + d\alpha_g)/(2R + d) \sim d\alpha_g/(2R + d)$. This value is substantially larger than

2.6×10^{-5} (1/K) along the c-axis of graphite. Because the thermal expansion is related to lattice anharmonicity, this result indicates that the anharmonicity in SWNT bundle is larger than that in graphite.

In the present analysis, it should be noted that the used values for the tube diameter and the lattice constant are "averaged" values over the sample and did not take account of the distribution.[12] Thus, the simulated patterns could not completely reproduce the observed ones. For example, the fitting around $Q \sim 0.8$ (1/Å) in Fig. 6 seems to be improved by taking into account the existence of the bundles with different tube diameters and lattice constants. However, we believe that such a more sophisticated treatment would give essentially the same thermal expansion coefficients as the present analysis.

In conclusion, the thermal expansion of the tube diameter and lattice constant were determined as $(-0.15 \pm 0.20) \times 10^{-5}$ (1/K) and $(0.75 \pm 0.25) \times 10^{-5}$ (1/K), respectively. The small coefficient for the tube diameter indicates the strong carbon-carbon bonds comparable to that of graphite. The thermal expansion coefficient for the intertubule gap is $(4.2 \pm 1.4) \times 10^{-5}$ (1/K), which is much larger than that of graphite, indicating the larger lattice anharmonicity.

*Present address: SPring-8, 1-1-1 Kouto Mikazuki-cho Sayo-gun Hyogo 679-5198, Japan.

[1] For reviews, *Carbon Nanotubes and Related Structures*, by P.J.F. Harris (Cambrige University Press, Cambrige, 1999); *Science of Fullerlenes and Carbon Nanotubes*, by M.S. Dresselhaus, G. Dresselhaus, and P.C. Eklund (Academic Press, New York, 1995).

[2] S. Iijima and T. Ichihashi, Nature (London) **363**, 603 (1993).

[3] D.S. Bethune, C.H. Kiang, M.S. de Vries, G. Gorman, R. Savoy, J. Vazquez, and R. Beyers, Nature (London) **363**, 605 (1993).

[4] A. Thess, R. Lee, P. Nikolaev, H. Dai, P. Petit, J. Robert, C. Xu, Y.H. Lee, S.G. Kim, A.G. Rinzler, D.T. Colbert, G.E. Scuseria, D. Tomanek, J.E. Fischer, and R.E. Smally, Science **273**, 483 (1996).

[5] C. Journet, W.K. Maser, P. Bernier, A. Loiseau, M. Lamy de la Chapelle, S. Lefrant, P. Deniard, R. Lee, and J.E. Fischer, Nature (London) **388**, 756 (1997).

[6] H. Kataura, Y. Kumazawa, Y. Maniwa, Y. Ohtsuka, R. Sen, S. Suzuki, and Y. Achiba, Carbon **38**, 1691 (2000).

[7] Y. Maniwa, Y. Kumazawa, Y. Saito, H. Tou, H. Kataura, H. Ishii, S. Suzuki, Y. Achiba, A. Fujiwara, and H. Suematsu, Jpn. J. Appl. Phys., Part 2 **38**, L668 (1999).

[8] Y. Maniwa, Y. Kumazasa, Y. Saito, H. Tou, H. Kataura, H. Ishii, S. Suzuki, Y. Achiba, A. Fujiwara, and H. Suematsu, Mol. Cryst. Liq. Cryst. **340**, 671 (2000).

[9] A. Fujiwara, K. Ishii, H. Suematsu, H. Kataura, Y. Maniwa, S. Suzuki, and Y. Achiba, Chem. Phys. Lett. **336**, 205 (2001).

[10] A.C. Bailey and B. Yates, J. Appl. Phys. **41**, 5088 (1970).

[11] Y. Maniwa, R. Fujiwara, H. Kira, H. Tou, E. Nishibori, M. Takata, M. Sakata, A. Fujiwara, X. Zhao, S. Iijima, and Y. Ando, Phys. Rev. B **64**, 073105 (2001).

[12] E. Anglaret, S. Rols, and J.L. Sauvajol, Phys. Rev. Lett. **81**, 4780 (1998).